Journal of Thermal Analysis, Vol. 5 (1973) 117—136

Special Reviews

THERMAL ANALYSIS OF POLYMERS

B. WUNDERLICH

Rensselaer Polytechnic Institute Troy, New York, USA

(Received March 29, 1972)

Results of research on the quantitative thermal analysis of polymers by calorimetry are reviewed. Adiabatic and scanning calorimeters are briefly described and data obtained are discussed in terms of current theories. Heat capacities, glass transition phenomena and melting of macromolecules are treated.

1. Experimental techniques*

The main problem in any type of thermal analysis is the fact that there are no perfect insulators for heat. Accordingly, thermal measurements must be continuously corrected for heat losses. In adiabatic calorimetry these heat losses are minimized by surrounding the calorimeter with a shield at almost the same temperature. The smaller the temperature difference can be kept between calorimeter and jacket, the smaller is the heat leak. A further subdivision of the adiabatic calorimetry can be made into isothermal and nonisothermal measurements.

Nonisothermal adiabatic calorimeters are most useful in the temperature range of up to 600°K, the temperature region of most interest for linear high polymer work. The basic design was developed by Nernst (1911). In principle, a metal calorimeter containing the sample, a heater, and a thermometer is supported in a jacket of large heat capacity of accurately measurable and controllable temperature. To reduce heat losses due to convection, jacket and calorimeter are contained in an insulated, evacuated container. Cooling can be done by liquid nitrogen or helium. The heating is done electrically. Small imbalances in temperature between calorimeter and jacket are measured and used for correction calculations. The temperature rise caused by the heat input is detected by a resistance thermometer. Accuracies as high as 0.01 % have been claimed. Routinely the order of magnitude of 0.1 % accuracy can be achieved.

Heat capacity measurements at temperatures below 10°K need some specialized instrumentation. The main problems rest with the cryostat and low temperature thermometry.

* General References [23, 37].

Isothermal calorimeters are mostly used for higher temperatures and of less importance for polymer specific heats. The principle is to thermostat the sample at a known high temperature and measure the total enthalpy loss of the sample on transfer to a low temperature isothermal recipient. The recipient low temperature calorimeter may be a Bunsen ice calorimeter, or an aneroid calorimeter. The resulting data are averages over large temperature ranges. The accuracy is usually somewhat less than in the non-isothermal calorimeter, although accuracies as high as 0.2% have been reported.

The adiabatic calorimeters described above can be termed classical precision calorimeters. Particularly in the polymer field it was noticed, however, that many samples were thermodynamically not stable enough to be measured discontinuously over long time periods. Only a continuous and fast heating mode can, in many cases, prevent irreversible changes of the sample during measurement. The search for fast heating dynamic calorimeters has led to the development of differential calorimeters. The adiabatic condition has been given up in favor of a heat leak of identical magnitude for sample and reference. The measurement is based on a linearly heated block into which sample and reference are placed with a thermal resistance, so that the temperature gradient within the sample is kept small. The temperature difference between block and sample is proportional to the heat flow into the sample, and the temperature difference between sample and reference in turn is a function of the difference in heat capacity between the two. This type of calorimeter is based on the well known differential thermal analysis. A commercial instrument has been developed using the same principle.* Its temperature range is 175 to 875°K. The heating rate is variable between 1 and 30°C min^{-1}, the sample mass between 1 and 200 mg. The claimed accuracy is 5% or better.

Another dynamic differential calorimeter has been described by O'Neill (1964). This instrument is also available commercially.** It differs slightly from the differential calorimeters above by keeping almost identical temperatures in sample and reference by automatic control. The differential heat input per second necessary to achieve this, $d\Delta Q/dt$, is monitored. Its value during heating with rate $q = dT/dt$ is proportional to the differential specific heats. The heating rates of the DSC range from 0.62 to 80°C min^{-1}. Sample weights are between 1 and 50 mg. Temperature lags caused by the physical separation of heater and sample can be estimated knowing the finite thermal resistance between sample and sensor. The published value of thermal resistance for the DSC is 100°C sec cal^{-1}. During melting, a sudden absorption of the heat of fusion unbalances the steady state reached on constant heating, and the lag increases. For a heat flow of 8 mcal sec^{-1} at 5°C min^{-1} heating rate, 1–2°C lags were found. Since the noise level is only 0.04 mcal sec^{-1}, the amount of polymer melting can be reduced to levels small

* duPont DSC-Cell used with the duPont 900 differential thermal analyzer, E. I. duPont de Nemours and Co., Inc. Instrument Division, Wilmington, Delaware.

** Differential Scanning Calorimeter, DSC, Perkin-Elmer Corp., Norwalk, Conn.

enough to give negligible lags. The accuracy of heat capacities on polymers is 1 to 2%. The reproducibility of standard compounds is as good as 0.5% [13].

In summary: adiabatic calorimeters of $\pm 0.1\%$ accuracy have been built for measurement of polymer heat capacities. Each of these calorimeters represent a large investment of time and money, since every instrument is custom built. Their operation is somewhat slow because of the need to equilibrate after every step, usually chosen between one and twenty degrees. The data resulting from these calorimeters forms the base of most of the following discussion. Recognizing the metastability of many polymer samples, and the differences due to thermal pretreatment, has led to the recent development of dynamic calorimeters with an accuracy of $\pm 1\%$ or less, which are commercially available and produce results much more effortlessly. The loss in accuracy is often compensated for by the high heating rate which avoids changes in structure of the sample during heating.

2. Heat capacity*

The heat capacity is the fundamental thermodynamic quantity out of which all other parameters can be derived:

$$\begin{array}{ll} \text{Enthalpy} & H = \int C_p dT \\ \text{Entropy} & S = \int (C_p/T) dT \\ \text{Free energy} & G = H - TS \end{array} \qquad (1)$$

The theory which links the heat capacity to the molecular motion is well developed, such that much information can be gained from its study.

Motion in the solid state consists mainly of vibrations of atoms around their respective equilibrium positions. These vibrations are usually assumed to be harmonic oscillations. The harmonic approximation allows the description of the state of motion in terms of normal modes. The molar heat capacity is simply the sum of the contribution of all normal modes:

$$C_v = R \sum E(\Theta/T) . \qquad (2)$$

$E(\Theta/T)$ represents the Einstein function which is the contribution of a single vibration to the heat capacity:

$$E(\Theta/T) = \Theta^2 [\exp(\Theta/T)]/[1 - \exp(\Theta/T)]^2 , \qquad (3)$$

Θ represents the Einstein temperature and is defined by:

$$\Theta = h\nu/k . \qquad (4)$$

R, k and h have the usual meaning, ν is the frequency, and T is the temperature. If the normal modes of vibrations are known, it is a simple matter to evaluate the heat capacity with the help of Eq. (2).

* General References [23, 28].

The chemical structure of a linear high polymer allows the separation of the normal modes of vibration into two categories. The first category are the group vibrations, the second category the skeletal vibrations. The skeletal vibrations can be looked upon as vibrations of a chain of beads with the appropriate masses. The group vibrations consist then of the normal modes of the detailed structure of the beads. Their contribution to heat capacity is given by the sum over the Einstein terms for each normal mode (Eq. (3)) multiplied by the number of beads. Much information on the group vibration can be gained from the infrared absorption spectra and from the study of low molecular weight compounds. A series of approximations have been proposed for the skeletal vibrations. A first approximation is to find the vibrational spectrum of the isolated chain. For long wave lengths or low frequencies it is possible to neglect the atomic structure of the chain and use a continuum approximation which leads to a constant frequency distribution. The heat capacity is in this case expressed by the one-dimensional Debye function and will be abbreviated by the symbol D_1:

$$C_v = 3RD_1(\Theta_1/T). \tag{5}$$

The one-dimensional Debye function has been tabulated [4]. This approximation should work best for the heat capacity of isolated chains at low temperatures and yields a linear temperature dependence of the heat capacity up to about $T/\Theta_1 = 0.1$. As the wave lengths of the vibrations become smaller and reach the order of magnitude of the distance between atoms, the continuum approximation breaks down. Calculation of the exact frequency spectrum of a string of beads, however, is not difficult. It leads to normal frequencies represented by:

$$\nu = \pm\nu_1 \sin(\pi L/N), \quad L = 1, 2, \ldots, N. \tag{6}$$

Here ν_1 is the maximum frequency and L represents a quantum number running from one to N, where N is the number of beads in the chain. Knowing the proportionality between ν and L, it is a simple task to derive the frequency distribution:

$$\rho(\nu) = 2N/\pi(\nu_1^2 - \nu^2)^{\frac{1}{2}}. \tag{7}$$

At low frequencies Eq. (7) is nearly constant as expected, at high frequencies the value of $\rho(\nu)$ increases steeply in contrast to the Debye approximation.

Although the forces between chains within a crystal are relatively weak, there is coupling between the vibrations of the different chains for low frequencies. Tarasov proposed to describe the skeletal heat capacities of linear high polymers in a second approximation as the sum of two contributions: D_3, a three-dimensional Debye function for the intermolecular vibrations, and D_1 a one-dimensional Debye function for the intramolecular vibrations:

$$C_v = 3R\{D_1(\Theta_1/T) - (\Theta_3/\Theta_1)[D_1(\Theta_3/T) - D_3(\Theta_3/T)]\}. \tag{8}$$

The high and low temperature regions of the heat capacity are to be fitted separately to one- and three-dimensional Debye functions. Since the constant frequency dis-

tribution of the intramolecular vibrations would be of use only at the lower frequencies where it is replaced by the three-dimensional frequency distribution, the Tarasov approximation must be looked upon as an empirical equation where all frequencies beyond the intermolecular vibrations are averaged in terms of a box frequency distribution. Because heat capacities are relatively insensitive to higher frequencies the Tarasov approximation has been used successfully for a number of polymers [23]. Table 1 shows a collection of data for Θ_1 and Θ_3 evaluated by the use of Eq. (8).

Table 1

Θ_1 and Θ_3 for skeletal vibrations of various polymers

Polymer	Θ_1, °K	A	B	Θ_3, °K
Polymeric selenium	370	—	—	97
Polyethylene	540	1.00	1.00	147
Polystyrene	230	0.50	0.43	41
Polypropylene	480	0.82	0.83	—
Polybutadiene	580	—	—	—
Polyisoprene	580	—	—	—
Polytetrafluoroethylene	270	0.53	0.50	46
Poly(vinylidene chloride)	260	0.54	0.48	—
Poly(vinyl chloride)	350	0.67	0.65	175

A = Square root of the ratio of mass per backbone carbon to mass of CH_2. B = Ratio of Θ_1 of the polymer in question to Θ_1 of polyethylene.

The Θ-values in Table 1 except for selenium are calculated for two normal vibrations per chain atom, since the third is related to the C–C stretching vibrations and was shown for polyethylene to consist of a narrow distribution which can be treated better with the group vibrations.

Vibrational frequencies are proportional to the square root of the force constant and inversely proportional to the square root of the mass. Comparing on this basis Θ-temperatures of polyethylene with other polymers of identical backbone chain shows that the Θ_1 temperatures are close to the ratio of the square root of the masses, while the Θ_3 values are not. As a result one must conclude that for example the intermolecular forces which govern the value of Θ_3 are much stronger in polyethylene than in polytetrafluoroethylene. The Θ_1 values in turn are, as long as the carbon–carbon backbone is similar in different polymers, largely determined by the mass per chain atom. In this dependence of Θ_1 of carbon–carbon backbone polymers on mass lies the justification of an addition scheme of heat capacities described below. Θ_3 governs the skeletal heat capacity only at the lowest temperatures while Θ_1 determines the skeletal heat capacity at higher temperatures. The group vibrations which make up the rest of the heat capacity are additive by their very nature. Strictly, this discussion applies only to the heat capacity at

constant volume. However, only at temperatures above room temperature does the contribution of $C_p - C_v$ become significant.

For most polymers a detailed frequency spectrum is not available. From the discussion of all data available to date [23] it became clear that differences in conformation, crystallinity, and intermolecular forces of carbon backbone linear high polymers are only of little importance above about 60°K. They become important again at the glass transition temperature and above because of different motion in amorphous and semicrystalline polymers. This leaves a relatively large temperature range between 60°K and the melting transition temperature where the differences in heat capacity between polymers are largely determined by the

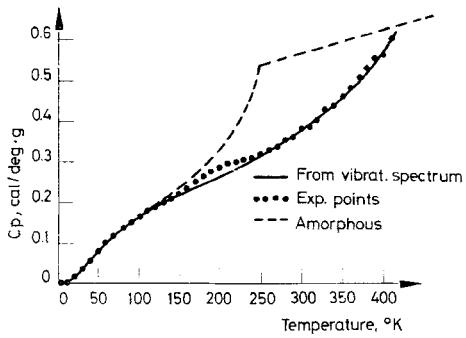

Fig. 1. Extrapolated heat capacities of completely crystalline polyethylene (lower curve) and completely amorphous polyethylene (upper curve). Up to 10°K the heat capacity is proportional to the third power of temperature. Above 10°K the heat capacity becomes accidently linear. At temperatures above 300°K a second increase of heat capacities due to optical vibration becomes noticeable

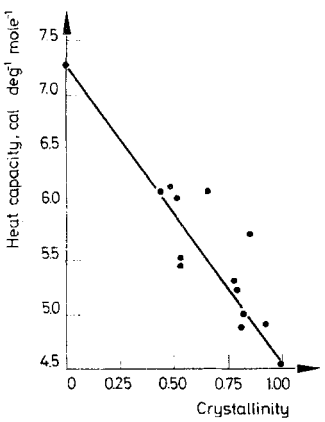

Fig. 2. Dependence of heat capacity of polyethylene on crystallinity at 260°K. The completely amorphous point represents the extrapolated heat capacity from the melt. The almost completely crystalline point represents measured heat capacities for 99% crystalline polyethylene

difference in mass per carbon backbone atom and the difference in group vibrations, a conclusion supported by the Θ_1-values of Table 1. Based on these findings it is possible that heat capacities in this temperature region can be derived by adding characteristic contributions arising from the different chemical groups in the polymer molecule. Tables of such contributions have been derived [28].

Experimental information about the heat capacity of completely crystalline polyethylene has been gathered in three ways. First, the heat capacities of polyethylene samples with different degrees of crystallinity were extrapolated to com-

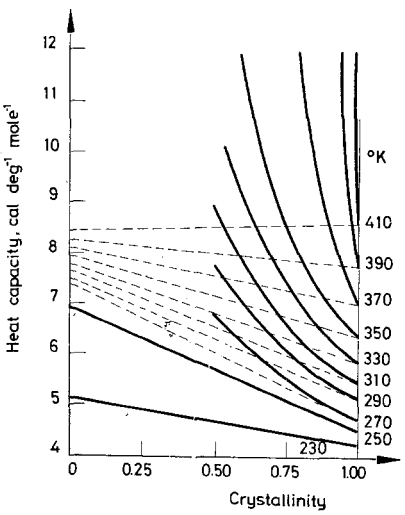

Fig. 3. Heat capacities of polyethylene as a function of crystallinity and temperature for the upper temperature region. The dashed lines represent hypothetical heat capacities if additivity of amorphous and crystalline heat capacity would exist. The curved lines indicate that in this region an additional contribution due to melting or defect reorganization can be found

plete perfection (see Fig. 2 and also [3]); second, the heat capacity of perfectly crystalline paraffins of increasing chain length was extrapolated to infinite chain length; and finally, the heat capacity of extended chain crystals was measured. All three methods gave agreement on the heat capacity [13]. Figure 1 reproduces the best data presently available for completely crystalline polyethylene up to the melting point. The deviations in the vicinity of the melting point are illustrated in Fig. 3.

The heat capacity curve deviates significantly from the simpler curves of metals for example. A cubic temperature dependence of the heat capacity is found up to only 10°K. Then the temperature dependence changes slowly such that an approximately linear portion exists between 110 to 210°K. This is followed by a levelling off, but only to be followed by a new rise in heat capacity starting at about 250°K. The heat capacity at 400°K is only $3.5R$ per mole of CH_2-units instead of $9R$ which would be expected for complete excitation of all vibrations.

The calculated frequency spectrum of polyethylene holds the key to all features of the heat capacity [4] in Fig. 1. Eq. (2) allows the calculation of the heat capacity and in fact, the drawn out curve in Fig. 1 has been calculated from the frequency spectrum. The initial correspondence T^3 dependence of heat capacity comes from the smooth initial increase in the number of vibrations with frequency (up to about 10^{12} cps). Several peaks interrupt this correspondence already at about 10–20°K. The linear portion finally comes about because of the almost flat portion in the frequency spectrum. The levelling off above 210°K is caused by the gap in possible frequencies at about $2 \cdot 10^{13}$ cps and the new rise comes from a series of vibrations between 2.2 and $4.4 \cdot 10^{13}$ cps. The very high frequencies do not contribute to the heat capacities at temperatures below 400°K. Even the intermediate group is excited only to a limited degree.

Since the frequency spectrum was evaluated by theoretical calculation as well as experimentation, it is possible to say more about the type of motion the atoms carry out [4, 23]. The lowest frequency series of vibration is mainly a skeletal vibration. The chain is contracting and expanding by bending the C–C–C bonds. The higher portion to $1.5 \cdot 10^{13}$ cps includes skeletal twisting vibrations. These two modes of vibration can contribute $2R$ to the heat capacity, a value which is reached at about 250°K. Above the gap, the so-called optical vibrations start. Their higher frequency is caused by a motion stretching the C–C bond which takes a much higher energy than bending or twisting it. The main portion of this group of frequencies, however, involves bending of C–H bonds. All together $5R$ would be contributed to the heat capacity if all these vibrations were excited. Since at 400°K only $3.5R$ is measured and $2R$ is contributed by the skeletal motion, these low optical vibrations are excited at this temperature to about 30%. The last series of vibrations are C–H stretching vibrations. Their frequency is very high because of a strong C–H bond and a small H mass. These vibrations could contribute $2R$ to the heat capacity. Calculations show that at 400°K they are no more than 2% excited.

Unfortunately polyethylene is the only polymer for which such detailed analysis is available. For most other polymers for which preliminary frequency calculations are available no experimental heat capacity data of sufficient quality and quantity are available.

3. The glass transition temperature

Only the molten state of linear high polymers can be called with some certainty an equilibrium state which is independent of thermal history. Its heat capacity is still caused, for the largest part, by molecular vibration. In addition, conformational changes and internal rotations are possible and need to be accounted for. In general, little is known about the detailed motion in the liquid state as it applies to the heat capacities. Only liquid polyethylene melt has been analyzed in some detail [9] as is shown in Fig. 4.

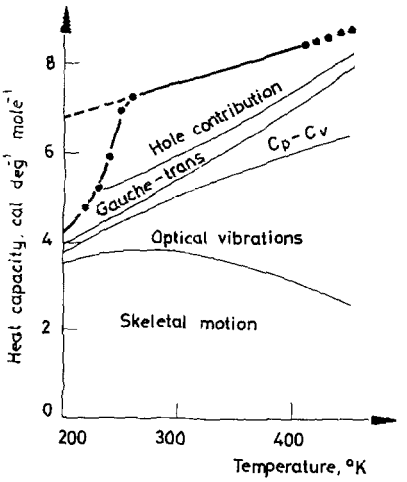

Fig. 4. Breakdown of the heat capacity of amorphous polyethylene. The glass transition temperature occurs at 237°K

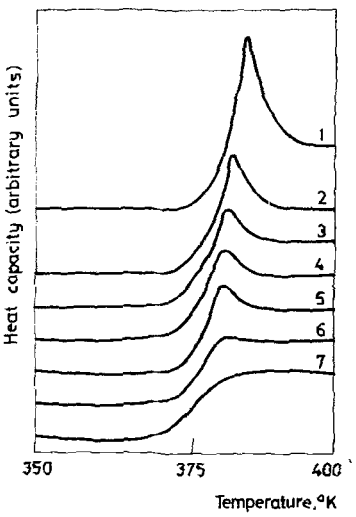

Fig. 5. Heat capacity of polystyrene as measured through the glass transition region by differential thermal analysis. The data had been corrected to zero temperature difference between reference and sample below the glass transition interval. All measurements were made at constant heating rates of $9.0 \cdot 10^{-2}$ °C/sec. The linear cooling rates: 1: $1.4 \cdot 10^{-4}$; 2: $3.2 \cdot 10^{-3}$; 3: $8.7 \cdot 10^{-3}$; 4: $1.8 \cdot 10^{-2}$; 5: $4.13 \cdot 10^{-2}$; 6: $8.7 \cdot 10^{-2}$ and 7: 0.5 °C/sec. Successive curves have shifted ordinates. The hysteresis maximum is observed in particular if the cooling rate is much less than the heating rate. An indication of a minimum is observable for very quickly cooled glasses

At lower temperatures, conformational changes slow down. The liquid becomes a glass. Only pendant groups and shorter size chains may remain mobile and freeze at a lower temperature. The temperature of the final freezing of large scale molecular motion is called the glass transition temperature. Since the motion slows down gradually, different conformations freeze in at different cooling rates. On reheating hysteresis phenomena can be observed in the heat capacity.

The apparent heat capacity of polymers in the glass transition range has been described as a function of heating and cooling rate [18]. As a simple starting point the hole theory of liquids as developed by Frenkel (1946) and Eyring (1936) was chosen. The process of hole formation is assumed in this theory to require a hole energy ε, to overcome the cohesive forces, and an activation energy ε_j, to overcome the activated state necessary for rearrangement. Furthermore, all holes have been characterized by one mean volume, v_h. A straightforward application of the transition state theory allows the description of the approach to equilibrium. As a given liquid is cooled, T_g, the glass transition temperature, defined as the temperature of half-freezing of the hole equilibrium, depends only on the rate of cooling, since the liquid is in an equilibrium state. In contrast, as a glass is heated, T_g depends not only on the heating rate, but also on the thermal history. Differently cooled glasses are different starting materials, which in turn have different enthalpies and accordingly different time-dependent heat capacities in the glass transition range. Fig. 5 shows the heat capacity of polystyrene in the glass transition range. The samples were cooled at different rates, but heated all at 0.09°C sec^{-1}. To express this behaviour of the heat capacity mathematically, the equilibrium number of holes at temperature T, $N^*(T)$ was represented by the Boltzmann relation:

$$N^*(T)v_h = N_0 v_0 \exp(-\varepsilon/RT) . \tag{9}$$

Below T_g, the glass does not have its equilibrium number of holes, but the approach to equilibrium is assumed to be proportional to the difference between $N^*(T)$ and the actual number N:

$$dN/dt = (1/\tau)\,[N^*(T) - N] ; \tag{10}$$

τ, the relaxation time, depends on temperature and can be expressed by transition state theory as:

$$\tau = (h/kT)\,(Q^h/Q^{\neq})\exp(\varepsilon_j/RT) , \tag{11}$$

h is Planck's constant, k Boltzmann's constant, and Q^h and $Q^{\neq}$ the partition functions of the hole and the activated state. Changing variables from time to temperature via the heating rate,

$$q = dT/dt \tag{12}$$

one arrives at the general equation for the number of holes:

$$N = N^*(T) - \exp[-\phi(T)]\left\{[N^*(T_a) - N_a]\int_{N^*(T_a)}^{N^*(T)} \exp[\phi(T)]\,dN^*(T)\right\} \tag{13}$$

$$\phi(T) = \int_{T_a}^{T} \frac{1}{q\tau}\, dT. \tag{14}$$

The subscript a refers to the initial condition of the glass, which in turn depends on its mode of formation, i.e., on cooling rate. Since this simplified treatment assigns every hole the same energy, the increase in specific heat at T_g due to hole formation is:

$$\Delta C_p = (\partial H/\partial T)_p \simeq \varepsilon(dN/dT) \tag{15}$$

so that the general rate dependent specific heat equation is:

$$\Delta C_p = \frac{\varepsilon}{q\tau} \exp\,[-\phi(T)]\left\{[N^*(T_a) - N_a] + \int_{N^*(T_a)}^{N^*(T)} \exp\,[\phi(T)]\, dN^*(T)\right\}. \tag{16}$$

Quantitative agreement between Eq. (16) and data of Fig. 5 was achieved. The maximum of Eq. (16) for a glass heated faster than it was cooled can be approximated by the relationship:

$$\log q = A - B/T_{max}. \tag{17}$$

A is approximately constant over 3 to 4 orders of magnitude of heating rate q, and B represents 0.4343 ε_i/R.

The drop in heat capacity in going from the liquid to the glass can be evaluated [7] by insertion of the equilibrium hole number into Eq. (15). Table 2 contains a list of ε_h and v_h for some polymers of known C_p.

Table 2

ε_h and v_h per mole of holes

Polymer	ε_h, cal	v_h, cm³
Polybutadiene	650	7.2
Polyethylene	740	7.6
Poly(methyl methacrylate)	750	8.9
Polyisoprene	930	10.5
Poly(vinyl chloride)	1000	11.6
Polyisobutylene	1000	12.4
Polystyrene	1600	21.9
Selenium	2800	2.4

For many glasses, polymeric and non-polymeric, ΔC_p calculated per mole of beads is about 2.7 cal deg^{-1}mole^{-1} [7]. These beads are the smallest sections of the solid that can move as a unit in internal rotation.

4. The melting transition

Different polymer crystal morphologies undergo different slow processes on heating. Equilibrium crystals with an extended chain conformation melt so slowly that more heat can easily be supplied to the crystals than can be used up in melting. Fig. 6 shows data on melting kinetics of polymethylene. In this experiment the interior of the crystals must superheat temporarily before melting. DTA and DSC have been used to analyze this melting process [10, 15, 16, 24, 32, 36]. Only little work has been done previously on the superheating of crystals in general and no

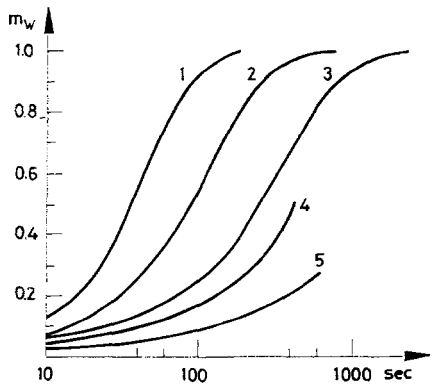

Fig. 6. Isothermal melting of extended-chain crystals of polymethylene. The fraction of polymer melted (m_w) is plotted as a function of the logarithm of time. 1: 148.5°C; 2: 146.5°C; 3: 144.5°C; 4: 143.5°C; 5: 141.5°C. The equilibrium melting point for this sample has been determined to be 141.4°C

calorimetry has been reported in the past. The analysis of polymer crystals is hampered by the fact that crystals are of different length in the chain direction as well as different width. It has not yet been possible to do experiments on isolated crystals. Qualitatively it could be proven that length as well as width influences superheating. For isothermal melting experiments plots of the amount still crystallized, w_c, versus the logarithm of time showed for most analyzed polymers an empirical relationship:

$$w_c = \exp(-t/\tau) \tag{18}$$

τ is a temperature dependent relaxation time. Fig. 7 shows a comparison of relaxation times of extended chain crystals of five different polymers as a function of superheating. The variation of the relaxation time with temperature seems to reach a limiting value of the order of magnitude of one second. How much of these values is size dependent and how much is a property of the polymer is not known at present.

Melting, reorganization, and recrystallization are three other processes possible in crystalline or semicrystalline polymers. As in glasses, the changes in enthalpy

due to conformation adjustment are more conspicuous than the changes in heat capacity due to vibrational mode rearrangement. The following effects have been observed by dynamic calorimetry:

1. The melting point decreases with increasing heating rate and stays constant at fast rates as illustrated in Fig. 8. This behavior is typical of reorganization on heating, which diminishes with increasing heating rate, such that finally a zero entropy production path with a direct melting of the metastable crystal to a supercooled melt is reached. This limit has been accomplished in well crystallized

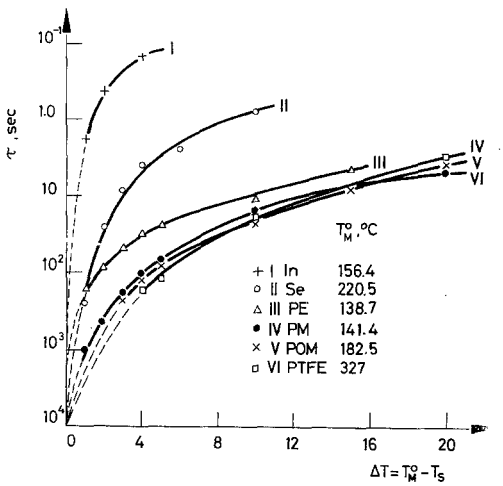

Fig. 7. Relaxation times of melting for a series of polymeric materials calculated according to Eq. (18). The data of indium were included to show the error limit of the instrument. Indium probably does not superheat

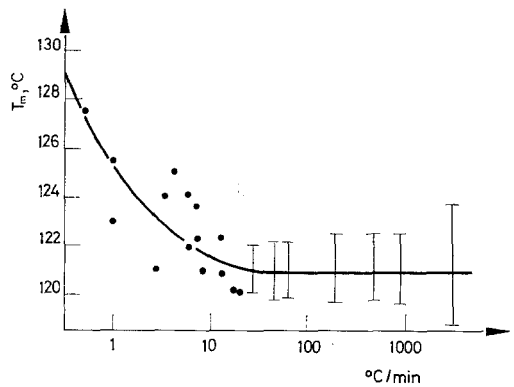

Fig. 8. Melting point of folded-chain polyethylene single crystals of approximately 130 Å fold length as a function of heating rate. The bars represent the limits of a large number of data collected at a particular heating rate

folded chain single crystals from solution at heating rates of 10–50°C/min. The zero entropy production limit can be used to get information on the surface free energy of these crystals.

2. The melting point stays constant with changing heating rates as shown in Fig. 9. More than one interpretation is possible if the melting point stays constant with changing rate for a completely unknown sample. *a)* This could be an equilibrium crystal which shows no superheating. *b)* This could be a metastable crystal with no rearrangement or recrystallization. *c)* The range of heating rates employed was too small and a compensation of superheating and reorganization occurred. Differentiation between *a*, *b* and *c* can be achieved by systematically varying crystallization conditions of the polymer in question.

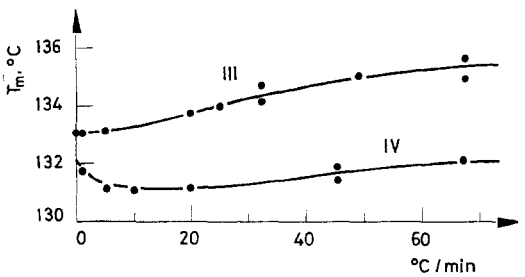

Fig. 9. Melting points of folded-chain polyethylene crystals grown from the melt measured as a function of heating rate. The points represent melting peaks measured by differential thermal analysis. The crystals of curve III were grown by cooling the melt at a rate of 0.6°C/min. Curve IV represents a melt cooled at 450°C/min. Curve III shows very little superheating. The melting point is almost constant. Curve IV shows some reorganization and then a constant melting

3. The melting temperature exhibits a maximum or minimum with changing heating rate. A combination of superheating and reorganization can give rise to such behavior. Since superheating changes mainly with crystal dimension in the molecular chain direction it is often not difficult to recognize this effect if any other information on the crystals is available (such as low angle X-ray data). Minima in melting temperature as a function of heating caused by rearrangement and superheating were found for polyethylene (Fig. 9, curve IV) and polytetrafluoroethylene [15]. A maximum in melting temperature can also be found [24] as a result of variable cold crystallization at different heating rates (Fig. 10, curve T_M^2). Cold crystallization is observed whenever quenched amorphous, or only partially crystalline sample is heated above its glass transition temperature slowly enough so that it can crystallize. Crystallization with a limited degree of reorganization of the molecular chains occurs in this case on heating. The lower the temperature of crystallization, the less perfect will be the resultant crystals, and the lower will be the melting point of the crystals produced on further heating. Faster heating rates will shift the crystallization temperature to higher levels and

thus increase the melting point of the resultant crystals. Increasing the heating rates to even higher levels, however, reduces the melting point again, because of insufficient time to complete cold crystallization. The overall result is a maximum in melting temperature with heating rate.

4. The melting experiments reveal multiple peaks as indicated by Figs 10 and 11. This situation can arise for several reasons. *a)* There may be crystals of two or

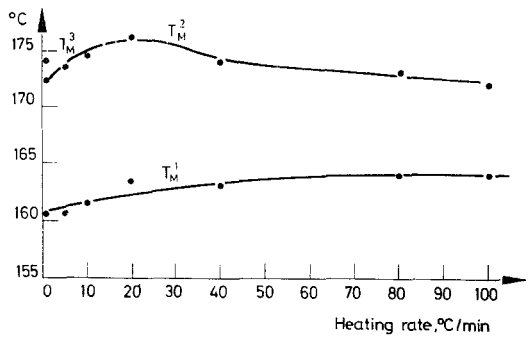

Fig. 10. Example of multiple melting peak temperatures. One of the melting curves as a function of heating rate exhibits a maximum. Differential thermal analysis of solution-grown folded chain polyoxymethylene hedrites. T_M2 and T_M3 represent the melting of more perfect polymer formed during the heating. On slow heating rates the material T_M2 is formed at lower temperatures and is consequently poorer. At heating of about 20°C/min. it reaches highest perfection. At faster heating rates not enough time is allowed for perfect recrystallization and the melting point T_M2 diminishes again. T_M3 was only observed for 1°C/min. heating. At faster heating not enough time is allowed for a second recrystallization. T_M1 represents the original melting of polyoxymethylene in hedrites

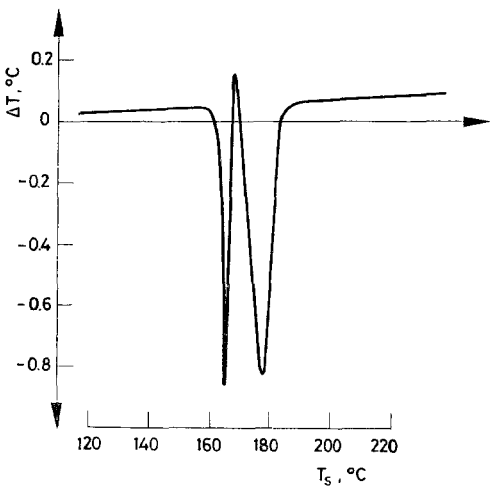

Fig. 11. DTA trace solution-grown polyoxymethylene hedrites measured at 10°C/min. heating rate (see also Fig. 10). This is an example of multiple melting peaks. Initial melting, recrystallization and melting of recrystallized polymer are clearly separated in this case

more degrees of perfection in the sample originally. Their study is helped by recrystallization on slow cooling, which produces usually only one of the crystal perfections for comparison. Heating the original sample at different heating rates must show an independent behavior of the differently perfect crystals. *b)* There may be reorganization of rather metastable crystals after partial or complete melting before final melting. In case of complete melting before crystallization, an endotherm can be observed by calorimetry before the final melting. Partial melting and crystallization may, however, go on simultaneously. In this case, a quantitative analysis of time dependent calorimetry can give further information. Increasing the heating rate will always decrease the amount of higher melting polymers, since the time left for recrystallization is shortened on increasing the heating rate. The separate melting peaks may vary irregularly in their temperature because of different reorganization times and temperatures at different heating rates (see Fig. 10 and [24]). *c)* There may be a portion of the polymer left amorphous or ill crystallized. On heating slowly, this amorphous or poorer crystallized material will crystallize (cold crystallization) or reorganize and melt at a different temperature from the crystals originally present. The amount of newly formed crystals during heating will decrease if heating rates are increased sufficiently, leaving at fast heating rates only the melting of the crystals originally present. *d)* Finally there may be a true phase transition from one crystal form to another before melting as is found, for example, in polytetrafluoroethylene and poly(1-butene), and is well known for low molecular weight substances.

The only well developed theory of melting is the thermodynamic theory. The heat capacity curve (Fig. 1) can form the basis of a thermodynamic description of the crystalline state. While the heat content measures the total thermal energy, the entropy is a measure of the order (higher entropy, lower order), and the free energy is a measure of the stability of the system in question (the equilibrium system always has the lowest free energy). Of interest also is the temperature coefficient of G:

$$(\partial G/\partial T)_p = -S\,. \tag{19}$$

This equation indicates that the system with higher entropy (lower order) has the largest temperature coefficient of the free energy (decreasing with increasing temperature). The free energy of the molten state must accordingly have a steeper slope than the free energy of the crystal because of the disordered molecular structure. At the sharp point of intersection both the melt and the crystal have the same free energy:

$$G_{melt} = G_{crystal}\,. \tag{20}$$

For the fusion process:

$$\Delta G_f = G_{melt} - G_{crystal} = 0\,, \tag{21}$$

and as a result comparing with Eq. (1):

$$\Delta H_f = T_m^\circ \Delta S_f \tag{22}$$

or

$$T_m^\circ = \Delta H_f / \Delta S_f \,. \tag{23}$$

ΔH_f and ΔS_f are the heat and entropy of fusion respectively, and T_m° is the equilibrium melting point. Eq. (23) contains the main result of the thermodynamic melting theory: The higher the heat of fusion (i.e. the larger the heat content difference between melt and crystal) and the lower the entropy of fusion (i.e. the smaller the difference in order between the melt and the crystal) the higher is the melting point.

Polymers have no high melting points due to large values of ΔH. In polymer melting no strong bonds are broken. Even if H-bonds are present as in the nylons, the heat of fusion remains low, leading to the conclusion that no significant number of the H-bonds are permanently broken during the melting process. The entropy of fusion can become relatively small, however, if a polymer has only limited flexibility. All high temperature polymers have stiff chains. If the melting point lies sufficiently high decomposition may occur before melting.

The second prediction of the thermodynamic theory is a sharply defined melting temperature. General experience, however, tells that polymers show a broad melting interval, only for extended chain polyethylene of high molecular weight has a sharp melting point been observed [11].

Equilibrium thermodynamics predicts a broader melting range for systems made up of more than one component. A two component system with both components miscible in the molten state may also show miscibility in the solid by formation of mixed crystals. If the two components are not miscible in the solid state a eutectic system results. For two components of about equal molecular size, the initial freezing point lowering in the eutectic diagram is described mathematically by:

$$\Delta T = \frac{RT^2}{\Delta H_{f_A}} \gamma_B \,; \tag{24}$$

γ_B is the mole fraction of the non-crystallizing component and H_{f_A} is the molar heat of fusion of the crystallizing component, so that Eq. (24) represents one side of the eutectic diagram. The exact equation of which Eq. (24) is a simplification for small γ_B and zero interaction, χ, is:

$$\Delta T = -RT_m T_m^\circ \left[\ln (1 - \gamma_B) + \chi \gamma_B^2\right] / \Delta H_{f_A} \,. \tag{25}$$

T_m and T_m° are the lowered melting point and the equilibrium melting point of the pure compound respectively. χ represents an interaction parameter correcting for non ideal behavior of the solution in the molten state. If the size of the molecules of the crystallizing solvent (2) and the non crystallizing solute (1) are different, Eq. (25) must be replaced by:

$$\Delta T = -RT_m T_m^\circ \left[\ln (1 - v_1) + (1 - x) v_1 + x v_1^2\right] / \Delta H_f \tag{26}$$

an equation derived by Flory and Huggins (1942). The main difference is that γ, the mole fraction is replaced by v, the volume fraction

$$v_1 = \frac{n_1 V_1}{n_1 V_1 + n_2 V_2}; \quad v_2 = \frac{n_2 V_2}{n_1 V_1 + n_2 V_2} \tag{27}$$

n_1 and n_2 are the numbers of moles of substances 1 and 2 in the mixture, V represents the corresponding molar volume. If the index 2 marks the larger molecule, the ratio of the molar volumes $V_2/V_1 = x$, so that x is a measure of the discrepancy between the molecular sizes. One can easily prove by insertion that for equal sizes $x = 1$, $v_2 = \gamma_B$ and Eq. (26) is equal to Eq. (25). A similar simplification for $x \gg 1$ is:

$$\Delta T = (RT^2/H_f)xv_1 . \tag{28}$$

Eq. (26) has been used extensively to calculate the interaction parameter and also heats of fusion of polymers. If applied to crystals which are not in equilibrium, Eq. (26) gives only questionable results.

One more application of Eq. (26) is the description of the equilibrium melting of extended chain homopolymer crystals with broad molecular weight distribution. To describe its melting curve one can assume initially that first the lowest molecular weight fraction melts. The next higher molecular weight portion will then have a lower melting point than in the pure state because of the presence of the lower molecular weight melt. Its melting point can be calculated using Eq. (26). As further portions melt, average values for x in Eq. (28) have to be evaluated. The proper way of averaging is to substitute x by:

$$\langle x \rangle = \sum n_i / \sum n_i x_i^{-1} .$$

n_i is the number of moles of molecules of length i in the melt, and x_i is the corresponding ratio of molar volumes. Above 410°K (137°C) the experimental points of polyethylene deviate from the calculated curve. An explanation for this is that the higher molecular weights do not form isolated crystals as assumed in deriving Eq. (26), instead they cocrystallize in mixed crystals. The thermodynamic analysis of this sample agrees well with the morphology of the crystals [19, 35].

In summary, the equilibrium polymer melting and crystallization is well understood. Homopolymers should crystallize or melt at a sharp temperature T_m°, determined by ΔH_f and ΔS_f. A broader melting (and also crystallization) range is expected for eutectic and mixed crystal forming systems. Special attention has to be paid to the size difference between the components. Non-equilibrium melting leads to the time dependent effects of superheating, recrystallization, and reorganization which can best be analyzed by differential thermal analysis.

References

1. B. WUNDERLICH and M. DOLE, J. Polymer Sci., 24 (1957) 201.
2. B. WUNDERLICH and M. DOLE, J. Polymer Sci., 32 (1958) 125.
3. B. WUNDERLICH, J. Chem. Phys., 37 (1962) 1203.
4. B. WUNDERLICH, J. Chem. Phys., 37 (1962) 1207.
5. B. WUNDERLICH, Polymer, 5 (1964) 125.
6. M. DOLE and B. WUNDERLICH, Makromol. Chemie, 34 (1959) 29.
7. B. WUNDERLICH, J. Phys. Chem., 64 (1960) 1052.
8. B. WUNDERLICH, Polymer, 5 (1964) 611.
9. B. WUNDERLICH, J. Chem. Phys., 37 (1962) 2429.
10. E. HELLMUTH and B. WUNDERLICH, J. Appl. Phys., 36 (1965) 3039.
11. T. ARAKAWA and B. WUNDERLICH, J. Polymer. Sci., Part C, 16 (1967) 653.
12. B. WUNDERLICH, J. Polymer Sci., Part C, 1 (1963) 41.
13. B. WUNDERLICH, J. Phys. Chem., 69 (1965) 2078.
14. B. WUNDERLICH and D. M. BODILY, J. Polymer. Sci., Part C, 6 (1964) 137.
15. E. HELLMUTH, B. WUNDERLICH and J. M. RANKIN, JR., Symposium Volume of the J. Appl. Polymer Sci., 2 (1966) 101.
16. B. WUNDERLICH and E. HELLMUTH, Thermal Analysis, Ed. J. P. Redfern, Macmillan and Co. Ltd., London, 1965, p. 76
17. B. WUNDERLICH and D. M. BODILY, J. Appl. Phys., 35 (1964) 95.
18. B. WUNDERLICH, D. M. BODILY and M. H. KAPLAN, J. Appl. Phys., 35 (1964) 95.
19. R. B. PRIME and B. WUNDERLICH, J. Polymer Sci., Part A-2, 7 (1969) 2073.
20. T. DAVIDSON and B. WUNDERLICH, J. Polymer Sci., Part A-2, 7 (1969) 2051.
21. B. WUNDERLICH and C. M. CORMIER, J. Polymer. Sci., Part A-2, 5 (1967) 987.
22. B. WUNDERLICH, L. MELILLO, C. M. CORMIER, T. DAVIDSON and G. SNYDER, J. Macromol. Sci.-Phys., B1 (1967) 485.
23. B. WUNDERLICH and H. BAUR, Fortschr. Hochpolymeren Forsch., 7 (1970) 151.
24. M. JAFFE and B. WUNDERLICH, Kolloid Z. Z. Polymere, 216–217 (1967) 203.
25. C. M. CORMIER and B. WUNDERLICH, J. Polymer. Sci., Part A-2, 4 (1966) 666.
26. F. LIBERTI and B. WUNDERLICH, J. Polymer Sci., Part A-2, 6 (1968) 833.
27. B. WUNDERLICH, Fortschr. Hochpolymeren Forsch., 5 (1968) 568.
28. B. WUNDERLICH and L. D. JONES, J. Macromol. Sci.-Phys., B3 (1969) 67.
29. B. WUNDERLICH, Angewandte Chemie, 80 (1968) 1009.
30. B. WUNDERLICH and L. MELILLO, Makromol. Chem., 118 (1968) 250.
31. T. DAVIDSON and B. WUNDERLICH, J. Polymer Sci., Part A-2, 7 (1969) 377.
32. M. JAFFE and B. WUNDERLICH, "Thermal Analysis" Vol. 1, R. F. Schwenker and P. D. Garn, Eds., Academic Press, New York, London, 1969, 387–403.
33. C. L. GRUNER, B. WUNDERLICH and R. C. BOPP, J. Polymer Sci., Part A-2, 7 (1969) 2099.
34. B. WUNDERLICH and T. DAVIDSON, J. Polymer Sci., Part A-2, 7 (1969) 2043.
35. R. B. PRIME and B. WUNDERLICH, J. Polymer Sci., Part A-2, 7 (1969) 2061.
36. R. B. PRIME, B. WUNDERLICH and L. MELILLO, J. Polymer Sci., Part A-2, 7 (1969) 2091.
37. B. WUNDERLICH, Differential Thermal Analysis in A. Weissberger and B. W. Rossiter Eds, Physical Methods of Chemistry, Vol. 1, Part V, Chapter 8, Wiley, 1971.
38. S. M. WOLPERT, A. WEITZ and B. WUNDERLICH, J. Polymer Sci., Part A-2, 9 (1971) 1887.
39. B. WUNDERLICH, Crystals of Linear Macromolecules. Academic Press, New York, 1972/73.

RÉSUMÉE — On passe en revue les résultats des recherches relatives à l'analyse thermique quantitative des polymères par calorimétrie. On donne une brève description des calorimètres adiabatiques et à compensation (DSC) et l'on discute les résultats obtenus en appliquant les théories courantes. On considère les chaleurs spécifiques, les phénomènes de transition vitreuse et la fusion des macromolécules.

ZUSAMMENFASSUNG — Eine Übersicht über die Forschungsergebnisse bezüglich der quantitativen thermischen Analyse von Polymeren mittels Kalorimetrie wird gegeben. Adiabatische und Scanning Kalorimeter werden kurz beschrieben und die erhaltenen Ergebnisse anhand der gegenwärtigen Theorien erörtert. Auf Wärmekapazitäten, Glas-Übergangserscheinungen und das Schmelzen von Makromolekülen wird ebenfalls eingegangen.

Резюме. — Изложены результаты количественного термического анализа полимеров методом калориметрии. Кратко описаны калориметры адиабатического и сканнирующего типов и полученные данные обсуждены на основе известных теорий. Рассмотрены теплоемкость, явления стеклования и плавления макромолекул